Materials International
Open-Access Journal (ISSN: 2668-5728)

Article
Volume 8, Issue 1, 2026, 7
https://doi.org/10.33263/Materials81.007

Synergistic Effect of ZnO Nanoparticles and Aspirin on the Electrochemical Behavior of Mild Steel in HCl

Msenhemba Moses Mchihi [1,*], Mercy Ezinwanyi Nwaubani [2], Bilqis Omobola Seriki [1]

[1] Department of Chemical Science, School of Science, Yaba College of Technology, Lagos, Nigeria;
[2] Department of Science Laboratory Technology, School of Science, Yaba College of Technology, Lagos, Nigeria
* Correspondence: mosesmsenhemba@gmail.com; msenhemba.mchihi@yabatech.edu.ng;

Received: 15.04.2025; Accepted: 27.07.2025; Published: 10.03.2026

Abstract: This study explores the synergistic effect of zinc oxide (ZnO) nanoparticles and aspirin on the corrosion of mild steel in 0.5 M HCl solution, using electrochemical impedance spectroscopy and potentiodynamic polarization. The observed shift in corrosion potential upon inclusion of the zinc oxide-aspirin (ZA) composite was below 85 mV, indicating mixed inhibition. Notably, the charge transfer resistance increased from 221 Ω cm² without the ZA composite to 1650 Ω cm² with a concentration of 0.4 g/L ZA, suggesting the formation of a protective ZA layer on the surface of mild steel. Furthermore, the corrosion current density showed a significant reduction, decreasing from 1698 µA cm^{-2} in the absence of ZA to 201 µA cm^{-2} with the addition of 0.4 g/L ZA. The extent of enhancement in charge transfer resistance (R_{ct}) and the reduction in corrosion current density (I_{corr}) in the presence of ZA were greater than those observed in a related study that employed ZnO nanoparticles alone. The adsorption of ZA to the surface of mild steel aligns with the principles of the Temkin model. ZA demonstrated potential as an effective corrosion inhibitor for mild steel in HCl.

Keywords: zinc oxide; acetylsalicylic acid; corrosion; acid; composite.

1. Introduction

Nanotechnology has undeniably opened up a range of new opportunities and developments in multiple scientific fields [1]. This advancement is largely due to the distinctive characteristics displayed by nanomaterials, particularly metal oxide nanoparticles. These characteristics encompass a heightened surface-to-volume ratio, variations in particle size, charge, optical, morphology, mechanical, and magnetic attributes, all of which distinguish them from their bulk forms [2,3]. Owing to its physical, chemical, thermal, and mechanical stability [4] at room temperature, ZnO nanoparticles are widely utilized in diverse fields such as corrosion mitigation [4-6], catalysis [7], sensing [8], and wastewater treatment [9]. In addition to its high chemical stability, the use of ZnO nanoparticles for metallic corrosion mitigation may be due to their high surface-to-volume ratio [10], excellent barrier properties, compatibility with many metal substrates, and high electron mobility [11].

The use of acids (such as hydrochloric acid) for pickling/descaling operations on mild steel (m-steel) often results in deterioration of m-steel due to the harsh nature of concentrated acids. Metal deterioration has caused significant economic losses worldwide. The significant

economic losses and accidents associated with metal deterioration have spurred the development of various techniques to mitigate metallic corrosion in acidic media. The use of corrosion inhibitors is one of the most effective and simple techniques for the mitigation of m-steel corrosion in acid media. ZnO nanoparticles act as corrosion inhibitors by forming a protective layer on metal surfaces, thereby restricting the infiltration of corrosive agents. This process encompasses the adsorption of nanoparticles onto the metal surface, facilitated by physical or chemical interactions, and may also exhibit synergistic effects when combined with other substances. Several researchers have reported the use of ZnO nanoparticles as corrosion inhibitors for metals in acidic media [4-6]. For instance, Elebo *et al*. [5] reported biosynthesis of ZnO nanoparticles for the mitigation of m-steel deterioration in HCl. The researchers achieved the highest inhibition efficiency of 78.30 % (from potentiodynamic polarization studies) and 79.11 % (from electrochemical impedance spectroscopy) when 0.5 g/L of ZnO nanoparticles was introduced into the corrosive HCl at room temperature [5]. Similarly, Al-Senani [4] synthesized nanoparticles of ZnO (with the aid of *Convolvulus arvensis* leaf extract) and studied their efficacy for protection against carbon steel deterioration. The findings from gravimetric and electrochemical investigations revealed that the synthesized ZnO nanoparticles exhibited appreciable inhibition efficiency and acted as a mixed-type inhibitor [4]. In their study, Pinto and Devadiga examined the impact of surface-modified zinc oxide nanoparticles on mild steel exposed to 0.5 M HCl at varying concentrations and temperatures using electrochemical techniques. The synthesized nanoparticles exhibited mixed inhibition behavior, achieving a maximum inhibition efficiency of 64% at a temperature of 40°C when 1000 ppm of the inhibitor was applied [1].

The majority of compounds that have shown significant efficacy in alleviating metal dissolution in various environments are composed of heteroatoms such as nitrogen, sulfur, and oxygen, along with π-electrons. These heteroatoms and π-electrons are known for their ability to create adsorption sites on the metal surface, leading to the formation of an inhibitor film that reduces the metal's vulnerability to aggressive media. A notable example of such compounds is aspirin, also known as acetylsalicylic acid. This crystalline substance is commonly employed as an analgesic, antipyretic, and anti-inflammatory agent. Its planar structure, which includes electron-rich oxygen atoms and π-electrons, enhances its potential for effective adsorption on metal substrates [11]. Aspirin has been reported to inhibit the deterioration of metals in an acidic medium. Ikeuba *et al*. studied the inhibitory potential of aspirin for mild steel deterioration in an acidic medium using both theoretical and experimental (i.e, hydrogen evolution) techniques. The highest observed inhibition efficiency reached 79.2% when 800 mg/L of aspirin was employed at a temperature of 333 K. In a related research study, the effectiveness of aspirin as a corrosion inhibitor for mild steel in 1 M hydrochloric acid was assessed within a temperature range of 303 to 333 K. The maximum inhibition efficiencies recorded were 77.58% and 77.91%, determined through potentiodynamic polarization and electrochemical impedance spectroscopy analyses, respectively [12].

Given the intriguing yet distinct characteristics of ZnO nanoparticles and aspirin, their amalgamation is likely to yield an enhanced protective effect against corrosion. When used in conjunction with another corrosion inhibitor, the collective inhibition efficiency substantially exceeds the sum of their individual contributions, resulting in a more effective anti-corrosion synergy than either constituent alone [13,14]. This occurrence is referred to as synergism. ZnO nanoparticles can adhere to metallic surfaces, forming a protective layer that resists corrosion. Meanwhile, the aspirin molecules can further reinforce this layer by chemically adsorbing to

the metal surface, thereby creating a more resilient protective barrier. Therefore, the aim of this study was to investigate the synergistic effect of ZnO nanoparticles and aspirin on the mitigation of m-steel deterioration in HCl. To the best of our knowledge, this has not been reported.

2. Materials and Methods

2.1. Electrochemical experiment.

Electrochemical analyses were conducted with the aid of Metrohm Autolab PGSTAT204 Potentiostat/Galvanostat. 2 g of acetylsalicylic acid (aspirin) were pulverized and mixed with 2 g of zinc oxide nanoparticles to obtain the inhibitor (i.e., ZnO nanoparticles/aspirin composite abbreviated as ZA). 0.5 M HCl was employed as the electrolyte. Electrochemical measurements were performed in the absence and presence of different concentrations of ZA (i.e., 0.1 g/L, 0.2 g/L, and 0.4 g/L).

To avert charging current and confirm system stability, open circuit potential (OCP) was recorded for a duration of 1800 seconds (30 minutes). This is required for the m-steel to dissolve at its equilibrium or free potential (E_{corr}), which is achieved at a stable OCP. Thereafter, all the electrochemical experiments were performed at OCP conditions. The electrochemical experiments were performed using a cell assembly consisting of 1 cm^2 exposed m-steel, which served as the working electrode, Ag/AgCl (which was utilized as a reference electrode), and platinum wire (which was employed as a counter electrode). Mild steel sheet comprising 98.835 Fe, 0.13 C, 0.025 Cu, 0.40 P, 0.18 Si, 0.04 S, and 0.39 Mn (wt.%) was employed for this study. All the reported potentials in this study are vs. Ag/AgCl. The electrochemical impedance spectroscopy (EIS) was performed with a signal amplitude perturbation of 10 mV throughout a frequency range of 100 kHz–10 mHz. The potentiodynamic polarization investigation was conducted in the potential range of ± 250 mV versus OCP at a scanning rate of 0.2 mV s^{-1}. The data were subsequently analyzed using appropriate electrochemical analytical software, such as Zsimpwin 3.2 for EIS, with the fitted equivalent circuit simulated for a specific m-steel/HCl environment, and EC-Lab was utilized for the potentiodynamic polarization analyses.

Equations 1 and 2 were utilized to calculate inhibition efficiency using PDP and EIS data, respectively [15].

$$\%IE = \frac{I°corr - Icorr}{I°corr} \times 100 \quad (1)$$

$$\%IE = \frac{Rct - R°ct}{Rct} \times 100 \quad (2)$$

Where R_{ct} stands for charge transfer resistance determined upon introduction of ZA, R^0_{ct} connotes charge transfer resistance in the absence of ZA, I^o_{corr} is corrosion current density obtained without ZA, whereas I_{corr} connotes corrosion current density obtained in the company of ZA.

3. Results and Discussion

3.1. Open circuit potential.

Open circuit potential (OCP) profiles of m-steel in an uninhibited 0.5 M HCl environment and different concentrations of ZA in a 0.5 M HCl harsh environment at room temperature are presented in Figure 1. The OCP versus time plots revealed a noticeable change

in OCP values obtained in bare HCl and in ZA-enriched HCl. The OCP became more positive upon the introduction of 0.1 g/L of ZA, suggesting that the presence of ZA has a great influence on the deterioration of m-steel in HCl. The shift of OCP towards more positive values further increased with a surge in inhibitor concentration. This observation is in agreement with other reports [15].

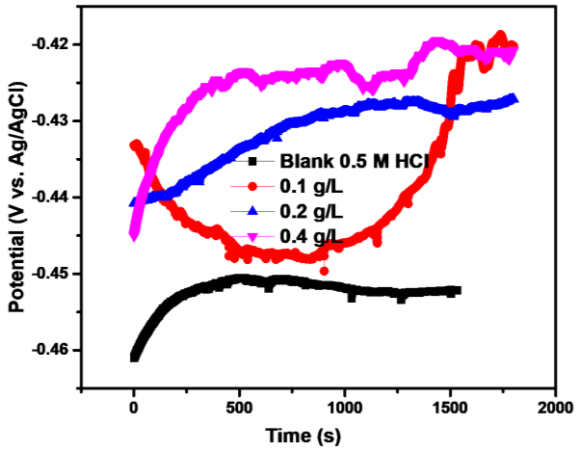

Figure 1. OCP versus time plots for mild steel in uninhibited HCl and different dosages of ZA in 0.5 M HCl.

3.2. Potentiodynamic polarization (PDP).

Potentiodynamic polarization is a widely used method for assessing corrosion resistance by varying the electrode potential. Polarization plots for mild steel in uninhibited HCl and different dosages of ZA in 0.5 M HCl are shown in Figure 2, from which the intersection of cathodic and anodic branches was analyzed to compute corrosion current (I_{corr}), Tafel slopes (βa and βc), and corrosion potential (E_{corr}). A drastic decrease in I_{corr} (from 1698 μAcm^{-2} to 702μAcm^{-2}) was observed upon introduction of 0.1 g/L ZA (Table 1). This considerable decrease in I_{corr} in the presence of ZA could be due to the adsorption of ZA on the m-steel surface, resulting in the formation of a protective ZA layer on the m-steel surface. This decrease in I_{corr} in the presence of ZA became more pronounced with a surge in ZA dosage, which could be due to an increase in the number of adsorbed ZA molecules. Consequently, inhibition efficiency (IE) and surface coverage (θ) also increased with a surge in ZA dosage. This observation is consistent with other reports [16-19]. The shift of values of E_{corr} obtained upon introduction of ZA relative to values of E_{corr} computed for m-steel in the bare HCl is less than 85 mV. This suggests that ZA exhibited mixed-type propensity [20]. The highest inhibition efficiency obtained in this study is higher than that reported in some studies that employed ZnO nanoparticles or aspirin alone [11,21,22].

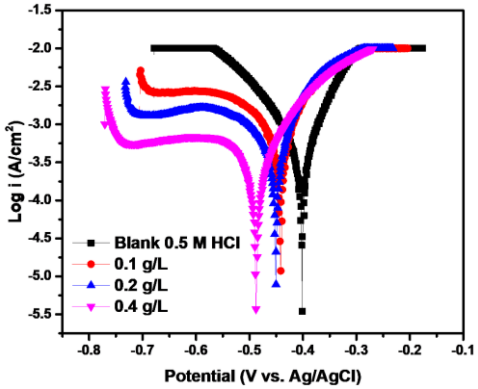

Figure 2. Polarization plots for mild steel in uninhibited HCl and different dosages of ZA in 0.5 M HCl.

Table 1. Potentiodynamic polarization (PDP) parameters for mild steel in uninhibited HCl and different dosages of ZA in 0.5 M HCl.

System	E_{corr}	I_{corr}	βa	βc	θ	IE
	mV/Ag/AgCl	μAcm^{-2}	$mVdec^{-1}$	$mVdec^{-1}$		%
Blank (HCl)	-400	1698	61	108	-	-
0.1 g/L	-425	702	63	110	0.587	58.7
0.2 g/L	-450	459	68	117	0.73	73.0
0.4 g/L	-475	201	71	125	0.882	88.2

3.3. Electrochemical impedance spectroscopy.

The equivalent circuit employed for fitting the impedance data is shown in Figure 3, while the electrochemical impedance spectroscopy (EIS) plot for m-steel in 1 M HCl, both in the absence and presence of ZA, is illustrated in Figure 4. R_s denotes solution resistance, R_{ct} is resistance to charge transfer, R_{po} represents pore resistance, and CPE refers to the constant phase element [10,16,23]. The data indicated the presence of two non-ideal capacitances (CPE1 and CPE2), attributed to the surface heterogeneity between the m-steel and protective layer. Notably, the semicircles observed are larger when ZA is present compared to those of m-steel in the uninhibited HCl, indicating the inhibitory effect of ZA [24-27]. The dimensions of the impedance diagrams increased with a corresponding surge in ZA dosage, thereby enhancing the protective efficiency. Additionally, the absence of deviations in the semicircular shapes observed in the presence of ZA suggests that the introduction of ZA did not modify the corrosion mechanism of m-steel in HCl. The presence of ZA boosted R_{ct} (Table 2) [20]. A consistent surge in R_{ct} and inhibition efficiency with ZA dosage was observed, which could be due to a surge in adsorbed ZA molecules on the m-steel surface. The increase in IE with an increase in inhibitor dosage is consistent with other reports [28]. The percentage inhibition efficiency (86.6%) obtained in the presence of 0.4 g/L ZA is greater than the inhibition efficiency obtained in the presence of 0.5 g/L of ZnO nanoparticles, as reported by Elebo *et al*. [5]. The magnitude of the increase in charge transfer resistance obtained in the presence of ZA is greater than that reported by Elebo *et al*. for ZnO nanoparticles. The Bode plots in Figure 5, illustrating the impact of ZA on the corrosion of mild steel in 0.5 M HCl, showed a larger area under the phase angle curves when ZA was present than in its absence. This significant increase is correlated with inhibitor concentration, as shown in the plots [29,30]. Specifically, an increase in the dosage of ZA resulted in a rise in the impedance modulus (at lower frequencies) and a corresponding increase in the phase angles [29]. This phenomenon may be attributed to an increase in R_{ct} due to the enhanced adsorption of inhibitor molecules onto the mild steel surface, leading to increased surface coverage and the formation of a protective film.

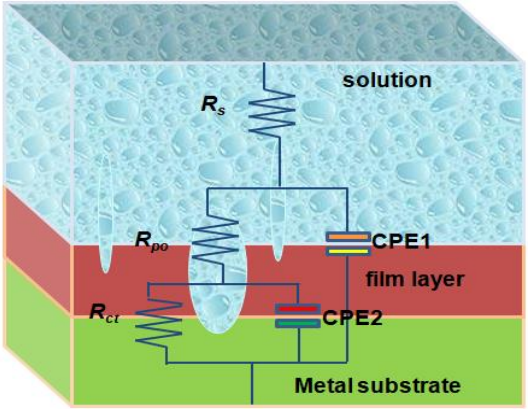

Figure 3. Electrochemical equivalent circuit fit for the blank, uninhibited, and inhibited samples at different concentrations, tested at room temperature.

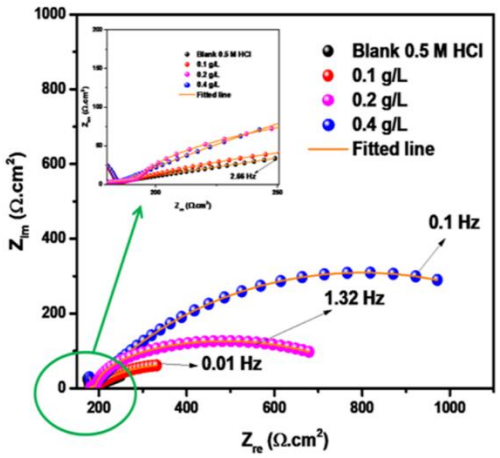

Figure 4. EIS plots for m-steel in uninhibited HCl and different dosages of ZA in 0.5 M HCl.

Table 2. EIS data for m-steel in uninhibited HCl and different dosages of ZA in 0.5 M HCl.

System	R_s	R_{po}	Q1x10^{-5}	n1	R_{ct}	Q2x10^{-5}	n1	θ	IE
	Ω cm^2	Ω cm^2	μΩ^{-1}s^n cm^{-2}		Ω cm^2	μΩ^{-1}s^n cm^{-2}			%
Blank (HCl)	20.00	15.3	51.03	0.87	221.01	12.00	0.86	-	-
0.1 g/L	19.30	20.6	54.00	0.87	430.0	11.6	0.88	0.486	48.6
0.2 g/L	18.99	15.3	56.3	0.87	810.0	9.1	0.89	0.727	72.7
0.4 g/L	19.65	20.5	58.1	0.88	1650.0	7.3	0.99	0.866	86.6

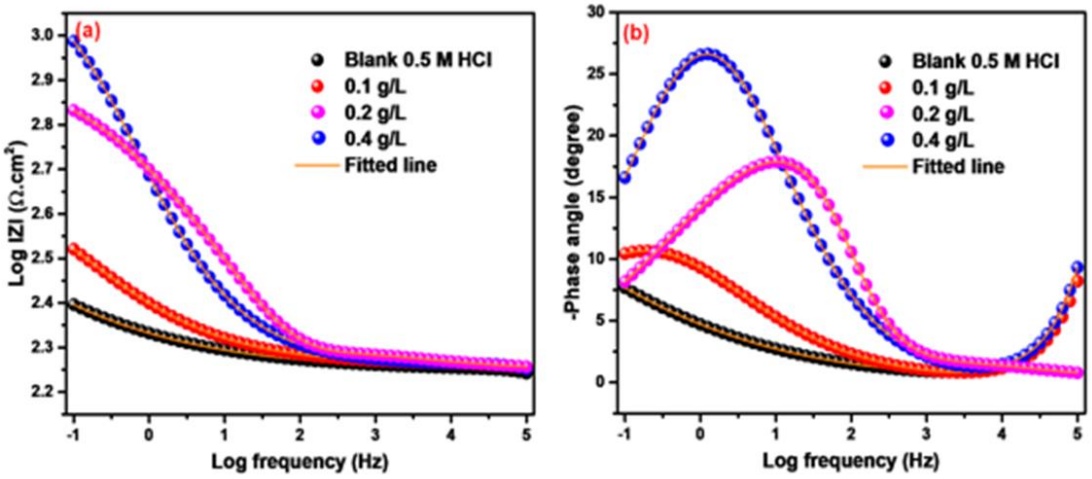

Figure 5. (a) Bode modulus plot; **(b)** phase angle plot for EIS analysis of mild steel in the company of ZA and without ZA in 0.5 M HCl.

3.4. Adsorption isotherm consideration.

Adsorption isotherm models play a vital role in corrosion research, as they facilitate an understanding of the interactions between corrosion inhibitors and metal surfaces. These interactions result in the formation of protective layers that mitigate corrosion by limiting the metal surface's exposure to corrosive agents. A range of adsorption isotherm models, including the Temkin, Langmuir, and Freundlich models, was employed to identify the model that best describes the interactions between the mild steel surface and the inhibitor adsorbent molecules. Specifically, the inhibitor concentration and surface coverage were used in accordance with Equations 3, 4, and 5, corresponding to the Temkin, Freundlich, and Langmuir models, respectively [31,32].

$$\theta \ -\frac{1}{2a} lnC - \frac{1}{2a} lnK \qquad (3)$$

$$\log\theta = logK + \frac{1}{n} logC \qquad (4)$$

$$\frac{C}{\theta} = C + \frac{1}{Kads} \quad (5)$$

Where C symbolizes the concentration of the inhibitors, K connotes the adsorption equilibrium constant, θ stands for the surface coverage, a denotes the molecular interaction parameter, and n is an empirical constant.

Table 3. Parameters obtained from adsorption isotherm studies.

Model	**Slope**	**Intercept**	**SD**	**R^2**
Temkin				
EIS	0.26029	1.12256	0.03459	0.99094
PDP	0.20908	1.06982	0.00417	0.99979
Langmuir				
EIS	3.69929	1.2515	2.08116	0.35847
PDP	3.56429	1.315	2.02317	0.35569
Freundlich				
EIS	3.7093	1.76347	0.85038	0.88043
PDP	0.28738	0.06021	0.00449	0.99933

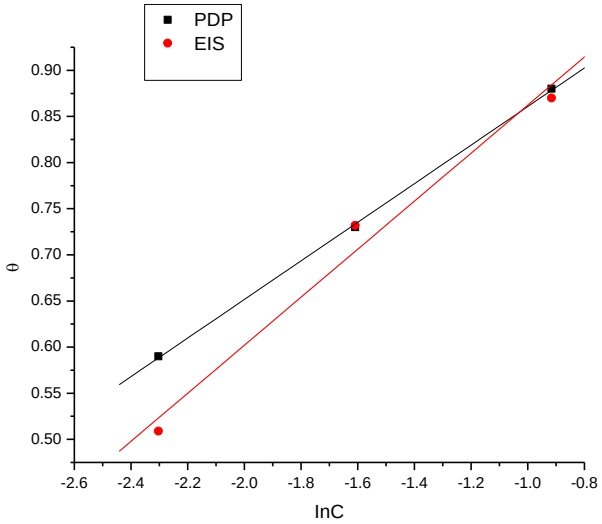

Figure 6. Temkin isotherm for the adsorption of ZA on m-steel in 0.5 M HCl.

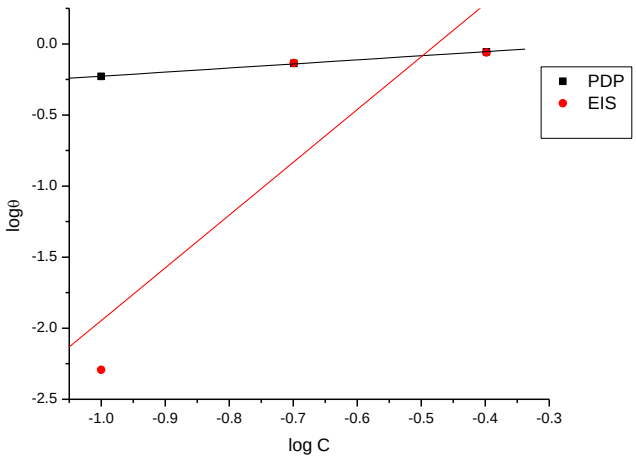

Figure 7. Freundlich isotherm for the adsorption of ZA on m-steel in 0.5 M HCl.

The extent of surface coverage was determined through electrochemical impedance spectroscopy and potentiodynamic polarization data. The resulting linear correlations between the degree of surface coverage (θ) and inhibitor concentration, illustrated in Figures 6, 7, and 8, along with the correlation coefficients (R^2) presented in Table 3, indicated that the Temkin

isotherm model provided the most accurate fit when compared to the Freundlich and Langmuir models [33,34]. This finding implies that the adsorption of the inhibitor onto the mild steel surface adheres to the principles of the Temkin model. This finding stands in contrast to certain studies that utilized ZnO nanoparticles solely as corrosion inhibitors. For example, in research by Al-Senani *et al*. [4] examining the effectiveness of ZnO nanoparticles in inhibiting carbon steel corrosion in hydrochloric acid, the adsorption of these nanoparticles onto the metal was found to align with the Langmuir model, as opposed to the Freundlich and Temkin models. Likewise, a study by Mchihi *et al*. [20] indicated that the adsorption of ZnO nanoparticles on the surface of m-steel was best described by the Langmuir model when compared to other isotherm models. This indicates that a synergistic effect may influence the adsorption characteristics of the corrosion inhibitors.

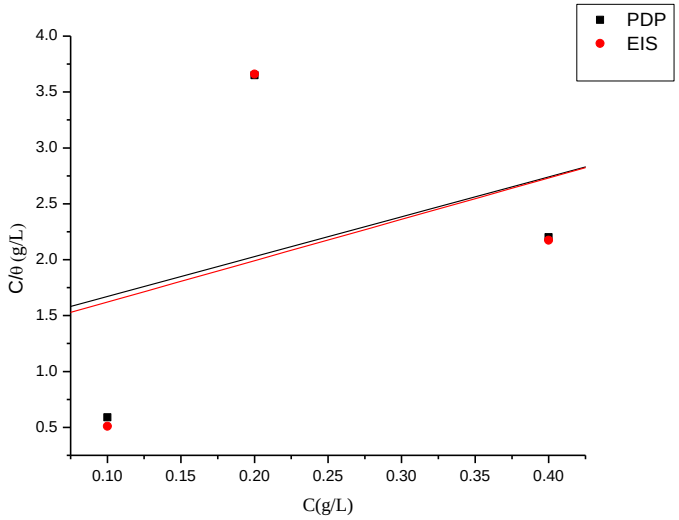

Figure 8. Langmuir isotherm for the adsorption of ZA on m-steel in 0.5 M HCl.

4. Conclusions

The zinc oxide-aspirin composite functioned as a mixed inhibitor. Importantly, the composite's presence led to a substantial increase in charge-transfer resistance. Additionally, the corrosion current density decreased markedly with the incorporation of the zinc oxide-aspirin composite. The degree of improvement in charge transfer resistance (R_{ct}) and the reduction in corrosion current density (I_{corr}) associated with zinc oxide-aspirin composite surpassed those reported in a related investigation involving ZnO nanoparticles alone for the reduction of mild steel corrosion in hydrochloric acid. Therefore, zinc oxide nanoparticles-aspirin composite appears to hold promise as an effective corrosion inhibitor for mild steel exposed to hydrochloric acid. Nonetheless, multiple avenues warrant further exploration to optimize, validate, and broaden the scope of this system's application. Future investigations might prioritize surface-sensitive methodologies, including X-ray Photoelectron Spectroscopy (XPS), Atomic Force Microscopy (AFM), and Transmission Electron Microscopy (TEM), to thoroughly examine the interaction mechanisms occurring between ZnO nanoparticles, aspirin, and the steel substrate at both atomic and molecular levels. Additionally, research may leverage computational approaches, such as density functional theory and molecular dynamics simulations, to clarify the mechanisms underlying the synergistic inhibition process. Systematic analyses aimed at identifying the optimal ratio of ZnO nanoparticles to aspirin to achieve peak inhibition efficiency will constitute another significant area of future research.

Author Contributions

Conceptualization, M.M.M.; methodology, M.M.M. and M.E.N.; software, M.M.M. and B.O.S.; validation, M.M.M., M.E.N., and B.O.S.; formal analysis, M.M.M.; investigation, M.E.N.; resources, M.M.M. and M.E.N.; data curation, M.M.M. and B.O.S.; writing—original draft preparation, M.M.M; writing—review and editing, M.M.M., M.E.N., and B.O.S; visualization, M.M.M.; supervision, M.M.M.; project administration, M.M.M., M.E.N., and B.O.S. All authors have read and agreed to the published version of the manuscript.

Institutional Review Board Statement

Not applicable.

Informed Consent Statement

Not applicable.

Data Availability Statement

Data supporting the findings of this study are available upon reasonable request from the corresponding author.

Funding

This research received no external funding.

Acknowledgments

The technical input of Dr. V. I. Chukwuike of Federal University of Health Science, Uburu, Ebonyi State, is acknowledged.

Conflicts of Interest

The authors declare no conflict of interest.

References

1. Pinto, G.M.; Devadiga, A. Development of silane functionalized ZnO nanoparticles for enhancing anticorrosion application. *Mapana J. Sci*. **2022**, *21*, 37-58.
2. Mchihi, M.M.; Olatunde, A.M.; Odozi, N.W. CuO-based nanocomposite: synthesis, characterization, and evaluation of the corrosion inhibition effectiveness for mild steel in HCl. *J. Electrochem. Sci. Eng.* **2025**, *15*, 2715, https://doi.org/10.5599/jese.2715.
3. Ulakpa, W.C.; Adaeze, I.M.; Chimezie O.A.; Olaseinde, A.A.; Odeworitse, E.; Onoriode, E.; Sarafa, O.A.; Olutoye, M.A.; Dim, P.; Siddique, M. Synthesis and characterization of calcium oxide nanoparticles (CaO NPS) from snail shells using hydrothermal method. *J. Turk. Chem. Soc*. **2024**, *11*, 825-834, https://doi.org/10.18596/jotcsa.1416214.
4. Al-Senani, G.M. Synthesis of ZnO-NPs Using a Convolvulus arvensis Leaf Extract and Proving Its Efficiency as an Inhibitor of Carbon Steel Corrosion. *Materials* **2020**, *13*, 890, https://doi.org/10.3390/ma13040890.
5. Elebo, A.; Sani, U.; Ekwumemgbo, P.A.; Ajibola, V.O. Green Synthesis and Zinc-Oxide Nanoparticles for Corrosion Inhibition and Modeling Corrosion Inhibition of Mild Steel in HCl Solutions. *Biosensors Nanotheranostics* **2024**, *3*, 1-17, https://doi.org/10.25163/biosensors.317339.

6. AL-Mosawi, B.T.; Sabri, M.M.; Ahmed, M.A. Synergistic effect of ZnO nanoparticles with organic compound as corrosion inhibition. *Int. J. Low-Carbon Technol.* **2021**, *16*, 429–435, https://doi.org/10.1093/ijlct/ctaa076.
7. Shamsuzzaman, Mashrai, A.; Khanam, H.; Aljawfi, R. N. Biological synthesis of ZnO nanoparticles using C. albicans and studying their catalytic performance in the synthesis of steroidal pyrazolines. *Arab. J. Chem.* **2017**, *10*, S1530–S1536, http://dx.doi.org/10.1016/j.arabjc.2013.05.004.
8. Al-darwesh, M.Y.; Ibrahim, S.S.; Naief, M.F.; Mohammed, A.M.; Chebbi, H. Synthesis and characterizations of Zinc oxide nanoparticles and its ability to detect O_2 and NH_3 gases. *Results Chem.* **2023**, *6*, 101064, https://doi.org/10.1016/j.rechem.2023.101064.
9. Haidri, I.; Shahid, M.; Hussain, S.; Shahzad, T.; Mahmood, F.; Hassan, M. U.; Al-Khayri, J. M.; Aldaej, M. I.; Sattar, M.N.; Rezk, A.A-S.; Almaghasla, M.I.; Shehata, W.F. Efficacy of Biogenic Zinc Oxide Nanoparticles in Treating Wastewater for Sustainable Wheat Cultivation. *Plants* **2023**, *12*, 3058, https://doi.org/10.3390/plants12173058.
10. Mchihi, M.M.; Odozi, N.W.; Gbolahan, S.A. Electrochemical investigation of the inhibitory effect of zinc oxide nanoparticles/tenofovir disoproxil fumarate nanocomposite on mild steel corrosion in 1 M hydrochloric acid. *Anal. Bioanal. Electrochem.* **2024**, *16*, 559-567, https://doi.org/10.22034/abec.2024.714079.
11. Ikeuba, A.I.; John, O.B.; Bassey, V.M.; Louis, H.; Agobi, A.U.; Ntibi, J.E.; Asogwa, F.C. Experimental and theoretical evaluation of Aspirin as a green corrosion inhibitor for mild steel in acidic medium. *Results Chem.* **2022**, *4*, 100543, https://doi.org/10.1016/j.rechem.2022.100543.
12. Prasanna, B.M.; Praveen, B.M.; Narayan Hebbar, Venkatesha, T.V.; Tandon, H.C.; Abd Hamid S.B. Electrochemical study on inhibitory effect of Aspirin on mild steel in 1 M hydrochloric acid. *J. Assoc. Arab Univ. Basic Appl*. Sci. **2017**, *22*, 62-69, https://doi.org/10.1016/j.jaubas.2015.11.001.
13. Wu, T.; Gao, B.; Zheng, Q.; Liu, S.; Wang, J. Corrosion Inhibition and the Synergistic Effect of Three Different Inhibitors on Copper Surface. *ECS J. Solid State Sci. Technol.* **2022**, *11*, 054009, https://doi.org/10.1149/2162-8777/ac6d75.
14. Wang, Q.; Zhao, C.; Zhang, Q.; Zhou, X.; Yan, Z.; Sun, Y.; Sun, D.; Li, X. Synergistic Effect of Benincasa hispida Peel Extract and KI on the Corrosion Inhibition of Mild Steel in HCl. *Sustainability* **2023**, *15*, 11370, https://doi.org/10.3390/su151411370.
15. Parangusan, H.; Sliem, M. H.; Abdullah, A. M.; Elhaddad, M.; Al-Thani, N.; Bhadra, J. Plant extract as green corrosion inhibitors for carbon steel substrate in different environments: A systematic review. *Int. J. Electrochem.* Sci. **2025**, *20*, 100919, https://doi.org/10.1016/j.ijoes.2024.100919.
16. Mchihi, M.M.; Odozi, N.W.; Nurudeen, A.O.; Emesiani, M.C.; Seriki, B.O. Assessment of Helianthus tuberosus leaves extract as eco-friendly corrosion inhibitor for Aluminum in sodium hydroxide: Insights from electrochemical, gravimetry and computational consideration. *Mor. J. Chem.* **2024**, *12*, 1462-1483, https://doi.org/10.48317/IMIST.PRSM/morjchem-v12i4.49160.
17. Kalu, O.D.; Nnanna, L.A.; Onyeije, U.C.; Asiegbu, A.D. Electrochemical Investigation of the Anti-Corrosive Effect of Spondias mombin Leaves Extract on the Corrosion of Aluminium Alloy (AA2024) and Mild Steel in 0.5 M NaCl. *Chem. Sci. Int. J.* **2023**, *32*, 44-51, https://doi.org/10.9734/CSJI/2023/v32i3847.
18. Odozi, N.W.; Emesiani, M.C.; Charles, C.D.; Seriki, B.O.; Mchihi, M.M. Electrochemical studies of the corrosion inhibitory potential of *Annona muricata* leaves extract on aluminum in hydrochloric acid medium. *FUDMA J. Sci.* **2024**, *8*, 39–401, https://doi.org/10.33003/fjs-2024-0803-2460.
19. Dadgarınezhad, A.; Baghae, F. Electrochemical Investigation of the Inhibitive Effect of a New Synthetic Schiff-base on the Corrosion of Mild Steel in Acidic Media. *Gazi U. J. Sci.* **2012**, *25*, 593–600.
20. Mchihi, M.M.; Olatunde, A.M.; Odozi, N.W. Ficus sur mediated synthesis of mesoporous ZnO nanoparticles and novel ZnO/Arginine/Tyrosine nanocomposite as eco-friendly corrosion inhibitors for mild steel in hydrochloric acid medium. *Mor. J. Chem.* **2024**, *12*, 931-1398, https://doi.org/10.48317/IMIST.PRSM/morjchem-v12i3.42782.
21. Akhir, R.M.; Norashikin, M.H.; Mahat, M.M.; Bonnia, N.N. Biosynthesis of zinc oxide nanoparticles for corrosion protection application. *Int. J. Eng. Technol.* **2019**, *7*, 488-492, https://doi.org/10.14419/ijet.v7i4.14.27775.
22. Odozi, N.W.; Mchihi, M.M.; Olatunde, M.A. Review of Recent Advances in Plant-Mediated Synthesis and Applications of $3d^6$ - $3d^{10}$ Metal Oxide Nanoparticles and their Composites. *DUJOPAS* **2023**, *9*, 91-120.
23. Al-Badour, F.A.; Adesina, A.Y.; Ibrahim, A.B.; Suleiman, R.K.; Merah, N.; Sorour, A.A. Electrochemical Investigation of the Effect of Process Parameters on the Corrosion Behavior of Aluminum-Cladded Pressure

Vessel Steel Using a Friction Stir Diffusion Cladding Process. *Metals* **2020**, *10*, 623, https://dx.doi.org/10.3390/met10050623.
24. Odozi, N.W.; Saheed, R.; Mchihi, M.M. Application of peperomia pellucida leaves extract as a green corrosion inhibitor for mild steel in 1.0 M hydrochloric acid solution. *ChemSearch J.* **2019**, *10*, 88 – 93.
25. Maduelosi, N.J.; Cookey, G.A.; Vopnu, T. Electrochemical Investigation Of The Corrosion Inhibition Of Mild Steel In 0.5 M HCl Using Napoleonae Imperialis Leaves Extract. *J. Appl. Chem*. **2024**, *17*, 47-52.
26. Odozi, N.W.; Adetoba, A.S.; Mchihi, M.M.; Akpaetok, A.N. Synsepalum dulcificum leaves extract as green inhibitor for mild steel corrosion in hydrochloric acid. *ChemSearch J.* **2021**, *12*, 47 – 54.
27. Gupta, S.K.; Mitra, R.K.; Yadav, M.; Dagdag, O.; Berisha, A.; Mamba, B.B.; Nkambule, T.I.; Ebenso, E.E.; Singh, S.K. Electrochemical, surface morphological and computational evaluation on carbohydrazide Schiff bases as corrosion inhibitor for mild steel in acidic medium. *Sci. Rep*. **2023**, *13*, 15108, https://doi.org/10.1038/s41598-023-41975-9.
28. Chioma, F.; Odozi, N. W.; Mchihi, M. M.; Olatunde, M. A. Synthesis, spectroscopic, and density functional theory studies of the corrosion inhibitive behaviour of *n*-(1,4-dihydro-1,4-dioxonaphthalene-3-yl)pyrazine-2-carboxamide chelator-ligand. *Global J. Pure Appl. Sci.* **2022**, *28*, 39-50, https://dx.doi.org/10.4314/gjpas.v28i1.6.
29. Abdallah, M.; Alfakeer, M.; Felaly, R.N.; Almohyawi, A.M.; Al-Fahemi, J.H.; Al-Juaid, S.S.; Seyam, D.F.; Mabrouk, E.M.; Soliman, K. A. Evaluation of porphyrin molecules as effective corrosion inhibitors for copper alloy in sulfuric acid using both experimental and computational approaches. *J. Electrochem. Sci. Eng*. **2025**, *15*, 2544, http://doi.org/10.5599/jese.2544.
30. Zhou, L.; Cheng, W.; Wang, D.; Li, Z.; Zhou, H.; Guo, W. The synergistic effect of 2-Chloromethylenzimidazole and potassium iodide on the corrosion behavior of mild steel in hydrochloric acid solution. *J. Electrochem. Sci. Technol*. **2022**, *13*, 138-147, https://doi.org/10.33961/jecst.2021.00682.
31. Loukili, E. H.; Kadda, S.; Azzaoui, K.; Bouklah, M. Adsorption of organic inhibitors on metal surface: isotherm models. *EHEI J. Sci. Technol.* **2023**, *3*, 95–107, https://doi.org/10.34874/PRSM.ehei-jst-vol3iss2.51336.
32. Mchihi, M.M.; Emesiani, M.C.; Babawumi, J. Inhibitory Potentials of Leaf Extract of Justicia schimperi for Mild Steel Corrosion in Hydrochloric Acid Medium: Gravimetric, Microscopic and Spectroscopic Studies. *ARJOCS.* **2023**, *5*, 184-192.
33. Koffi, A.A.; Coulibaly, S.; Yeo, M.; Coulibaly, K.K.; Niamien, P.M. Delving Ethyl 2-Oxo-2H-Chromene-3-Carboxylate as a Corrosion Inhibitor for Aluminum in Acidic Environments. *Orient. J. Chem.* **2025**, 41, 57-65, http://dx.doi.org/10.13005/ojc/410106.
34. Fouda, A.S.; Abd El-Maksoud, S.A.; El-Sayed, E.H.; Elbaz, H.A.; Abousalem, A.S. Experimental and surface morphological studies of corrosion inhibition on carbon steel in HCl solution using some new hydrazide derivatives. *RSC Adv.* **2021**, *11*, 13497–13512, https://doi.org/10.1039/d1ra01405f.

Publisher's Note & Disclaimer